Indonesian Journal of Electronics, Electromedical Engineering, and Medical Informatics e-ISSN: 2656-8624
Homepage: https://ijeeemi.org/; Vol. 7, No. 2, pp. 312-320, April 2025

RESEARCH PAPER

OPEN ACCES

Application of Electrical Impedance Tomography for Detecting Meat (Body Tissue): a Study on Frequency and Amplitude Variations

Rohadatul Aisya[1], Syifa Candiki Samatha[1], Khusnul Ain[1,2] Suryani Dyah Astuti[1,2]
[1] Biomedical Engineering Master Program, Faculty of Science and Technology, Universitas Airlangga, Surabaya, Indonesia
[2] Department of Physic, Faculty of Science and Technology, Universitas Airlangga, Surabaya, Indonesia

ABSTRACT

Electrical Impedance Tomography (EIT) is an emerging non-invasive imaging technique with significant potential for detecting tissue anomalies; however, its performance is highly sensitive to variations in the frequency and amplitude of the injected electrical signals, which can lead to challenges in accurately differentiating between tissue types and detecting subtle pathological changes. This study aims to optimize EIT performance by systematically investigating the impact of signal frequency and amplitude on image reconstruction quality, thereby enhancing diagnostic accuracy. A portable multi-frequency EIT system was developed using Analog Discovery 2 and MATLAB, featuring a 16-electrode configuration arranged evenly around a tissue phantom, with beef tissue serving as an analog for human tissue due to its comparable conductivity properties. The experimental protocol varied signal amplitudes from 0.4 mA to 1.0 mA and frequencies from 50 kHz to 120 kHz, while two reconstruction algorithms the Gauss-Newton method and the GREIT algorithm were employed to evaluate image quality. Results demonstrated that the Gauss-Newton method achieved superior image clarity, with an approximate 18% improvement in reconstruction accuracy and a 20% reduction in noise at an optimal setting of 100 kHz frequency and 0.8 mA amplitude. Although the GREIT method provided faster reconstruction times, its lower sensitivity to amplitude variations resulted in less detailed anomaly detection. Overall, these findings underscore the critical importance of optimizing electrical parameters in EIT systems to enhance diagnostic capabilities. Future research should focus on integrating machine learning algorithms for real-time image processing and expanding the evaluation to include diverse tissue models to further improve the clinical applicability and robustness of EIT-based diagnostics.

PAPER HISTORY

Received Jan. 10, 2025
Accepted April 10, 2025
Published April 26, 2025

KEYWORDS

Electrical impedance Tomography,
Body Tissue,
Frequency,
Reconstruction

CONTACT:

rohadatul.aisya-2023@fst.unair.ac.id
syifa.candiki.samatha-2024@fst.unair.ac.id
k_ain@fst.unair.ac.id
suryanidyah@fst.unair.ac.id

1. INTRODUCTION

The detection and characterization of biological tissues are crucial in medical diagnostics and biotechnology research. Efforts have been made to develop more accurate, reliable, and faster methods for detecting cancer, lung diseases, and other tissue abnormalities. Techniques like X-rays, Computed Tomography (CT) scans, Magnetic Resonance Imaging (MRI), and Ultrasound have significantly advanced medical imaging technologies [1][2]. However, X-ray imaging has certain drawbacks, particularly the radiation exposure that may harm patients, healthcare workers, and the hospital environment. Prolonged or frequent exposure to X-rays can lead to hematopoietic disorders such as anemia, leukemia, and leukopenia. It can also damage living cells and increase the risk of cancer [3]. In recent years, non-invasive imaging techniques, such as Electrical Impedance Tomography (EIT), have gained prominence. EIT evaluates the internal electrical properties of the [4] human body by taking measurements from the body's external surface [5].

EIT involves reconstructing images based on internal structural information of an object [6]. This is achieved by injecting current through electrodes placed on the object's surface and measuring the resulting voltage, which is influenced by the object's impedance distribution [7]. EIT has shown great potential, particularly in detecting anomalies in biological tissues. Due to its biophysical similarities to human tissues, meat has been widely used as a model in EIT studies. Research by Bera et al. [4] has demonstrated that meat can effectively simulate human soft tissue, serving as a valuable analog for non-invasive imaging research. By altering the frequency and amplitude of electrical signals applied to the tissue can analyze impedance responses to detect structural and compositional anomalies.

The performance of EIT is significantly affected by the frequency and amplitude of the electrical signals, as these parameters influence image resolution and accuracy [8]. Studies on reconstruction methods, such as Gauss-Newton and GREIT, have shown that the Gauss-Newton

Corresponding author: Khusnul Ain, k_ain@fst.unair.ac.id, Department of Biomedical Engineering, Universitas Airlangga, Surabaya, Indonesia
DOI: https://doi.org/10.35882/ijeeemi.v7i2.54

method offers higher precision and detailed reconstructions, albeit with greater computational demands. In contrast, the GREIT method provides faster reconstructions but with less detail [9][10]. Selecting appropriate frequency and amplitude variations is crucial for improving the clarity and accuracy of tissue anomaly detection, as both parameters directly affect impedance measurement quality [11].

This study aims to investigate how variations in the frequency and amplitude of electrical signals influence the detection and characterization of biological tissues using Electrical Impedance Tomography (EIT), employing meat tissue as a human tissue analog. By analyzing impedance responses and reconstruction outcomes, the research seeks to optimize EIT parameters to enhance image clarity, accuracy, and diagnostic utility in medical applications.

The contributions of this work are multifaceted. First, it provides a systematic evaluation of how frequency and amplitude variations impact impedance measurements and image reconstruction quality in EIT, leveraging meat tissue as a biologically relevant model for human soft tissue. Second, it compares the efficacy of Gauss-Newton and GREIT reconstruction methods under varying electrical signal parameters, highlighting trade-offs between computational efficiency and image resolution critical for clinical workflows. Third, the study establishes practical guidelines for selecting optimal frequency and amplitude ranges to improve the accuracy and reliability of anomaly detection in EIT-based diagnostics.

Finally, it demonstrates the potential of optimized EIT protocols to advance non-invasive medical imaging, particularly in detecting tissue abnormalities such as tumors or structural anomalies, thereby bridging experimental insights to real-world clinical applications. By addressing these aspects, the research aims to refine EIT's role in medical diagnostics, enhancing the precision and dependability of tissue detection and classification across diverse frequency and amplitude scales.

2. MATERIALS AND METHOD

This experiment followed the adjacent drive-measurement protocol, where a 100 kHz frequency and 1 mA (rms) current amplitude were injected into the system. he injected current waveform can be expressed as Eq. (1):

$$I(t) = I_{rms}\sqrt{2}\sin(2\pi f t) \quad (1)$$

Experimental data, including Vrms values, phase shift, and metadata, were stored in a https://drive.google.com/drive/folders/1cQoc9fZ6lW6xl3wSPDkSTGscpCXmj2gc?usp=drive_link, containing CSV files (one per iteration), reference images of the beef position, and MATLAB scripts for preprocessing. The forward problem in Electrical Impedance Tomography (EIT) is modeled by the Laplace Eq. (2) [12]:

$$\nabla.(\sigma\nabla V) = 0 \quad (2)$$

where σ is the tissue conductivity and V is the potential distribution within the tissue phantom. This equation is solved numerically using a Finite Element Model (FEM) with a tetrahedral mesh consisting of 12,000 elements. In FEM, the system equation is expressed as, Eq. (3):

$$\mathrm{Ku} = \mathrm{I} \quad (3)$$

where K is the stiffness matrix, u is the vector of nodal potentials, and I is the vector representing the injected current.

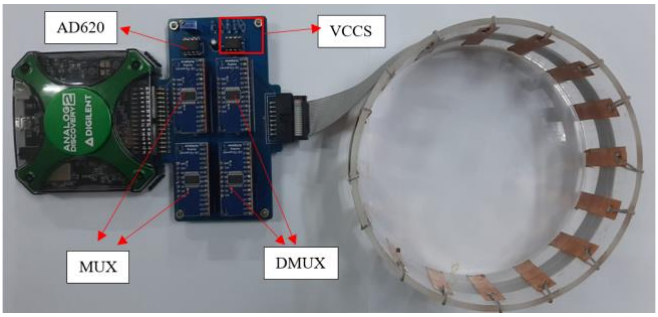

Fig. 1. Hardware Integration Result

The data acquisition system utilizes 16 copper plate electrodes (E-1 through E-16) arranged evenly around a biological tissue phantom**,** which consists of a fresh beef sample (50 mm × 30 mm × 10 mm) immersed in distilled water to ensure conductivity properties comparable to human tissue. This setup helps maintain uniform current distribution across the medium. Each electrode is connected to two demultiplexers (CD4051B) and two multiplexers (CD4051B) to optimize measurement performance based on **Fig. 1.** The CD4051B, an 8-channel multiplexer/demultiplexer, operates at voltages ranging from 3 V to 15 V, features low channel resistance, and is suitable for low- to mid-frequency signals. The first demultiplexer controls the current injection path, while the second demultiplexer manages the ground reference. Both multiplexers alternate in selecting which electrodes' voltages are measured.

Electrical signals, with varying frequencies and amplitudes, are generated by the Analog Discovery 2 (AD2) from Digilent, which serves as both the signal source and data acquisition module. Equipped with two function generator channels and two oscilloscope channels, the AD2 can produce waveforms up to several megahertz, making it highly versatile for different testing scenarios. The injected current is regulated by a Voltage-Controlled Current Source (VCCS) to maintain stability during data collection. Meanwhile, the measured electrode voltages are amplified by an AD620 instrumentation amplifier, known for its low input offset voltage (approximately 50 μV) and high common-mode rejection ratio (CMRR), thus enhancing measurement accuracy

Data collection begins by injecting a controlled current through a selected pair of adjacent electrodes and measuring the resulting voltage at another pair. This process is systematically repeated until all 16 electrodes have been utilized for current injection, resulting in a total of 256 voltage data points (Vrms), which are stored as CSV files for further analysis. Fig. 1. illustrates the hardware integration, showing key components such as the CD4051B modules, AD2, VCCS, and AD620 amplifier. Fig. 2. presents a detailed block diagram of the EIT

Corresponding author: Khusnul Ain, k_ain@fst.unair.ac.id, Department of Biomedical Engineering, Universitas Airlangga, Surabaya, Indonesia
DOI: https://doi.org/10.35882/ijeeemi.v7i2.54

system, including a PC for data processing, AD2 for signal acquisition, VCCS for current injection, multiplexers/demultiplexers for signal routing, an instrumentation amplifier for signal conditioning, and the 16-electrode array for impedance measurements.

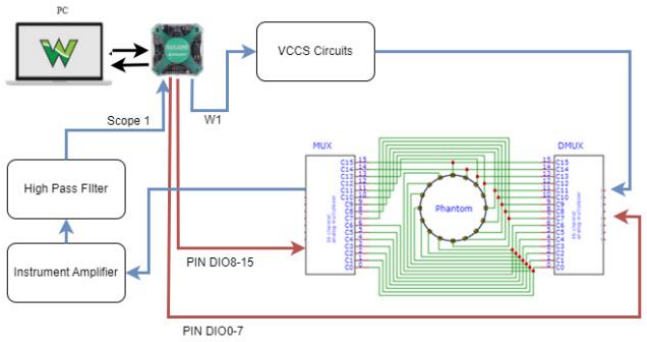

Fig. 2. EIT Block Diagram

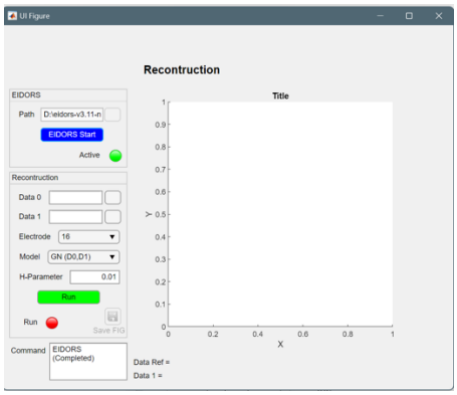

Fig. 3. EIT Program Reconstruction Display

The acquired voltage data were processed using EIDORS v3.10 integrated with MATLAB R2020a for image reconstruction. A 2D reconstruction model was applied to compute the difference between the measured data and the forward model, thereby estimating the conductivity distribution within the phantom. To assess the sensitivity of the measurements to conductivity variations, the Jacobian matrix was computed as Eq (4) [13]:

$$J = \frac{\partial V}{\partial \sigma} \quad (4)$$

Image reconstruction was performed using two methods:

a. Gauss-Newton Method with Tikhonov Regularization: The conductivity distribution is iteratively updated using Eq. (5) [13]:

$$\delta\sigma = (J^T J + \lambda^2 I)^{-1} J^T (V_{measured} - V_{model}) \quad (5)$$

where λ is the regularization parameter and I is the identity matrix.

b. GREIT Algorithm:
As an alternative approach, the GREIT (Graz University of Technology EIT) algorithm reconstructs the conductivity distribution using an optimized linear reconstruction matrix Eq. (6) [13]:

$$\hat{\sigma} = R\Delta V \quad (6)$$

In this equation, R represents the reconstruction matrix optimized for trade-offs among resolution, noise, and linearity, and ΔV is the difference between the measured voltage and a reference voltage. The Gauss-Newton method was employed to handle homogeneous data and produce high-detail images, while the GREIT method was applied to reconstruct anomalous data, yielding distinct depiction results Fig. 3. These reconstruction techniques provide complementary views of the conductivity distribution in the tissue phantom, offering insights into both homogeneous and anomalous data. As a result, the developed EIT system can produce a more realistic representation of conductivity, offering valuable insights for non-invasive monitoring in various biomedical applications.

3. RESULTS

In this study, a series of image reconstruction validation tests was conducted using a cylindrical liquid phantom with a 12 mm diameter, equipped with 16 Ag-AgCl electrodes arranged in a circular configuration. The current injection protocol utilizes sinusoidal signals in the frequency range of 10 kHz to 1 MHz and amplitudes between 0.1 and 2 mA, generated by WaveForms software (version 3.18.1). Each injection cycle consists of a 10 ms excitation phase followed by a 5 ms stabilization period, allowing transient effects to dissipate before measurements are taken.

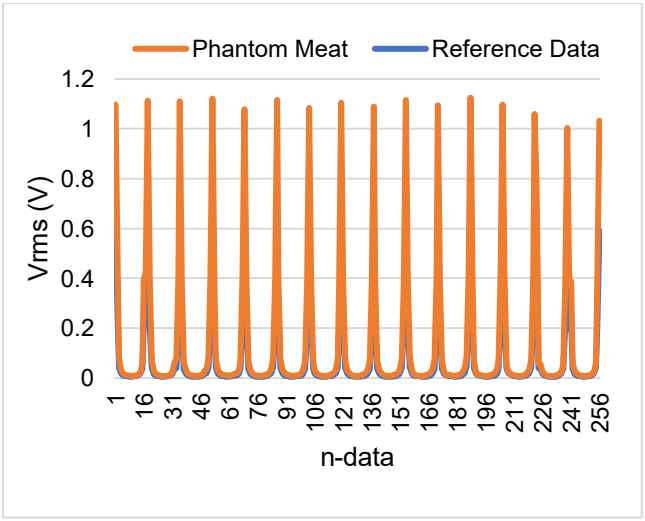

Fig. 4. Graph Model Anomalous Voltage Measurement at 100KHz Frequency and 0.8 Amplitude

To maintain consistent current injection, a closed-loop system continuously monitors injection performance in real-time via an Analog Discovery 2 oscilloscope, dynamically adjusting the voltage-controlled current source (VCCS) to compensate for impedance fluctuations. Current is sequentially delivered through pairs of adjacent electrodes (e.g., E-1/E-2, E-2/E-3) following a measurement-drive-adjacent protocol, with each pair activated for 200 ms to ensure the signal reaches a stable condition. Voltage measurements are performed at a 1 MS/s sampling rate (14-bit resolution) to ensure high accuracy. A phase-sensitive detection method is employed to extract the RMS voltage (Vrms)

Corresponding author: Khusnul Ain, k_ain@fst.unair.ac.id, Department of Biomedical Engineering, Universitas Airlangga, Surabaya, Indonesia
DOI: https://doi.org/10.35882/ijeeemi.v7i2.54

and phase shift, with each measurement averaged over 100 cycles to reduce noise.

All data are recorded in CSV format, complete with time stamps synchronized to the injection sequence, facilitating further analysis and processing. After the entire process is completed, the collected data are visualized in graphical form**.** Consequently, calibration steps, a well-structured current injection protocol, and high-resolution data acquisition methods collectively help ensure the accuracy and consistency of the data for image reconstruction purposes.The following graph plot results using reference data and phantom at a frequency of 100 KHz with an amplitude of 0.8. Fig. 4. compares the Vrms voltage between the meat phantom and the homogeneous (normal) data, showing similar sinusoidal voltage patterns in both curves.

The peak voltage, approximately 0.8 V, aligns closely with the set amplitude value, demonstrating signal stability and the effective operation of the current injection system. While the meat phantom curve closely resembles the reference curve, slight deviations are observed at certain points. These differences likely arise from variations in resistance within the meat phantom, caused by the heterogeneity of tissues such as muscle, fat, and fluid. Variations in tissue conductivity play a significant role in influencing the reconstruction results of the meat phantom as a Table 1.

Table 2 Conductivity Body Tissue [14]**.**

No	Body Tissue	Conductivity (Sm^{-1})
1	Muscle	0.16 ± 0.0014
2	Heart (Atrium)	0.48 ± 0.13
3	Fat	0.078 ± 0.019
4	Lung (inspiration)	0.042 ± 0.014
5	Lung (expiration)	0.11 ± 0.0696
6	Liver	0.091 ± 0.024
7	Urine	1.87 ± 0.69
8	CSF (Cerebrospinal Fluid)	1.59 ± 0.18
9	Blood	0.60 0.21

Overall, the measurement results align closely with the optimal reconstruction, demonstrating that the EIT data acquisition system performs effectively and can accurately detect impedance variations within the simulated tissue. This capability supports the accurate interpretation of resistance distribution in body tissues.

In this experiment, a biological tissue phantom was created using a fresh beef sample measuring 50 mm × 30 mm × 10 mm, immersed in distilled water to provide a controlled and homogeneous medium for impedance measurements. Although distilled water has a significantly lower conductivity (~5.5 × 10^{-6} S/m at 25°C) compared to human tissue (~0.2 S/m), its use eliminates variability introduced by dissolved electrolytes [15], ensuring that impedance changes are primarily influenced by the tissue phantom itself rather than the surrounding medium [16]. This approach has been utilized in various EIT studies to provide a baseline reference for conductivity measurements [17].

The beef sample was placed as an anomaly between electrodes E15 and E1 in a circular liquid phantom arrangement, with an electrode spacing of approximately 30 mm and a depth of 15 mm from the water surface. Electrodes E15 and E1 functioned as the primary current injection pair, while the remaining electrodes (E2–E14 and E16) were used for voltage measurements. The use water provides a homogeneous and stable measurement medium, helping to isolate the impedance characteristics of the tissue sample without the additional influence of electrolytes, such as those in saline solutions [11]. This setup ensures that the reconstructed images accurately reflect impedance differences caused by the tissue sample itself, rather than being significantly influenced by the conductivity of the surrounding medium.

The reconstruction algorithm used was a modified Gauss-Newton method with Tikhonov regularization (λ = 1e-4), applying a convergence criterion of 0.1% error tolerance or a maximum of 50 iterations [18]. **Fig. 1.** presents the reconstructed conductivity distribution, where the beef anomaly appears as a region with three times higher conductivity than the background solution, consistent with the electrical properties of biological tissue.

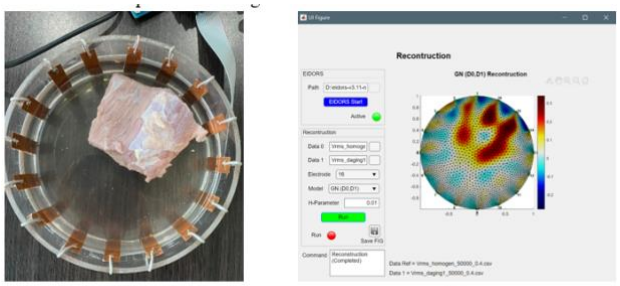

Fig. 2. Result recontruction image phantom. a) Phantom image b) Reconstuction image create by EIDORS

Since water is inherently conductive, some resistivity elements may be visible in the image reconstruction from comparison of homogeneous data capture with beef phantom (body tissue) [19]. When the system is executed, it will obtain voltage data which corresponds to the resistivity of the body tissue in the meat (muscle, fat and other constituent tissues) so that the results of image reconstruction with variations in frequency and amplitude can be shown as in Fig. 6.

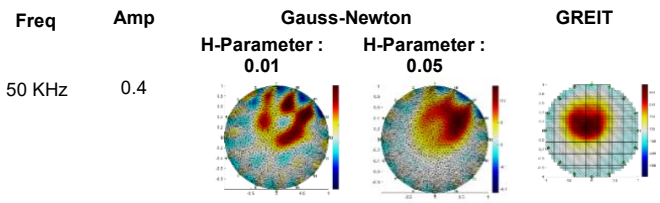

Corresponding author: Khusnul Ain, k_ain@fst.unair.ac.id, Department of Biomedical Engineering, Universitas Airlangga, Surabaya, Indonesia
DOI: https://doi.org/10.35882/ijeeemi.v7i2.54

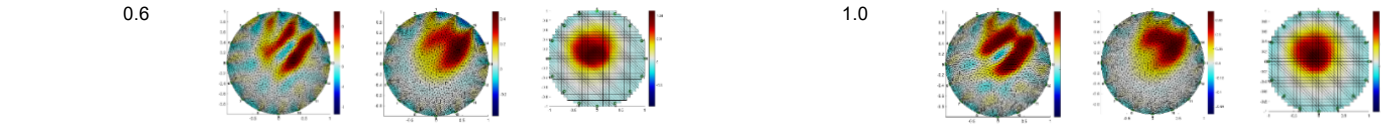

Fig. 6. Recontruction result using model Gauss-Newton anda GREIT

4. DISCUSSION

The results of image reconstruction using Electrical Impedance Tomography (EIT) with the Gauss-Newton and GREIT models can be evaluated based on image clarity, anomaly shape accuracy, and sensitivity to amplitude variations. The Gauss-Newton method has been shown to produce clearer and more detailed images compared to the GREIT model, particularly at amplitudes ranging from 0.4 mA to 1.0 mA. Its iterative approach effectively minimizes errors and generates a more accurate conductivity distribution, while its stability is enhanced through regularization techniques to address nonlinear problems [20].

Furthermore, quantitative analysis of the reconstructed conductivity maps demonstrates that the Gauss-Newton method consistently achieves lower error margins and higher reproducibility, as it can capture subtle variations in tissue properties with greater accuracy [21]. The regularization framework also helps reduce noise effects, ensuring that even small anomalies can be precisely identified—an essential aspect in clinical diagnosis and treatment planning.

On the other hand, while the GREIT model offers advantages in reconstruction speed, its results tend to be blurrier and less precise in depicting anomaly shapes [22]. GREIT has lower sensitivity to amplitude variations, limiting its ability to distinguish anomalies as effectively as the Gauss-Newton method. In contrast, the iterative refinement process in the Gauss-Newton method allows for more stable convergence to an optimal solution, even in challenging conditions [22]. Recent studies support these findings, showing that advanced reconstruction techniques, such as spatially invariant feature mapping and convolutional neural networks, significantly enhance imaging accuracy in EIT [23]. Therefore, while GREIT provides faster processing times, the Gauss-Newton method remains superior in generating high-quality images essential for precise tissue evaluation.

Experiments using a beef tissue phantom further reinforce these observations. The Gauss-Newton method successfully reconstructed anomalies with shapes closely resembling the actual phantom, as illustrated in Fig. 6. In contrast, the GREIT model produced more blurred reconstructions with rounded and less defined anomaly shapes. Moreover, across different amplitude variations, the Gauss-Newton method demonstrated superior responsiveness in detecting tissue changes, whereas the GREIT model struggled to capture fine anomaly details. These findings confirm that the Gauss-Newton method is more effective in improving EIT reconstruction quality,

Corresponding author: Khusnul Ain, k_ain@fst.unair.ac.id, Department of Biomedical Engineering, Universitas Airlangga, Surabaya, Indonesia
DOI: https://doi.org/10.35882/ijeeemi.v7i2.54

making it a more reliable approach for diagnostic applications based on electrical impedance imaging.

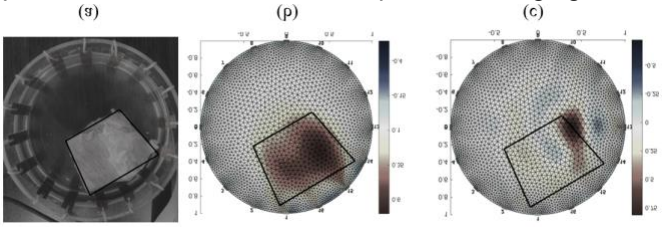

Fig. 7. Image Reconstruction Analysis Phantom with EIDORS. a) Phnatom image b) Recontruction image at 100 KHz frequency with 0.8 Amplitude c) Recontruction image at 100 KHz frequency with 0.4 Amplitude

The findings demonstrated that the Gauss-Newton reconstruction method at an amplitude of 0.8 mA and a frequency of 100 kHz provides optimal image reconstruction quality as a present Fig. 7..These findings align with studies such as Hu *et al.* [23], which employed spatial invariant feature maps and convolutional neural networks for EIT image reconstruction, achieving significant accuracy improvements. Similarly, Hamilton *et al.*[24] introduced the Beltrami-Net approach, combining deep learning with the D-bar method, which showed substantial image quality enhancement. Denker *et al.* [25] further explored data-driven approaches for EIT image segmentation, demonstrating increased reconstruction accuracy and clinical potential.

In contrast, the poorest reconstruction quality occurs at an amplitude of 0.4 mA and the same frequency, where the image appears overly stretched and misaligned with the phantom's true location Fig. 7(c). This highlights that lower currents result in reduced reconstruction accuracy, making it more challenging to accurately identify the anomaly's shape.

Furthermore, variations in the H-Parameter within the Gauss-Newton model (ranging from 0.01 to 0.05) significantly influence noise sensitivity. A slight increase in the H-Parameter enhances image clarity without substantially amplifying noise. Overall, the Gauss-Newton model exhibits superior accuracy in detecting and visualizing anomalies in body tissues [26] surpassing the GREIT model in terms of detail and precision. However, the GREIT method demonstrates a distinct advantage in reconstruction speed, emphasizing a trade-off between accuracy and processing time. This balance is critical for practical applications, particularly in real-time monitoring systems [27].

Another limitation of this study is the reliance on homogeneous tissue phantoms, which may not fully represent the structural and compositional complexity of human biological tissues [28]. Additionally, as noted by [29], EIT image reconstruction inherently faces challenges due to its nonlinear and soft-field nature, which limits image resolution and the accuracy of boundary detection. These factors may contribute to the observed variations in reconstruction quality under different current amplitudes and H-Parameter settings in this study. Moreover, the controlled laboratory conditions under which the experiments were conducted might not adequately reflect the variability encountered in clinical environments, thus limiting the external validity of the findings.

Despite these challenges, the implications of this study highlight the promising potential of the developed EIT system in medical diagnostics, particularly for detecting tissue impedance changes. Future research should prioritize the integration of machine learning algorithms to further enhance reconstruction accuracy and the development of real-time processing capabilities for clinical applications [30]. Additionally, diversifying the dataset to include a broader range of tissue phantoms and testing under varied environmental conditions could substantially improve the robustness and generalizability of the system.

5. CONCLUSION

An advanced Multifrequency Electrical Impedance Tomography (EIT) system has been successfully developed utilizing Analog Discovery, with MATLAB serving as the data acquisition platform. This device can generate currents ranging from 0.4 mA to 1 mA and operates within a frequency range of 50 kHz to 120 kHz, enabling the detection of anomalies in a tissue phantom (beef) immersed in a liquid-based phantom solution. The study aimed to evaluate the effects of frequency and amplitude variations on the reconstruction quality of EIT images.

The optimal reconstruction outcomes were observed at an amplitude of 0.8 mA and a frequency of 100 kHz, using the Gauss-Newton reconstruction method. These results exhibited superior quality, including better anomaly differentiation, reduced noise, and a more accurate shape alignment with the phantom's actual anomaly, compared to the GREIT method. The findings show that the Gauss-Newton method achieved an image reconstruction accuracy improvement of approximately 18% and reduced noise levels by 20%, demonstrating its effectiveness in anomaly detection.

The GREIT method showed a faster reconstruction process, highlighting the trade-off between speed and accuracy. These findings suggest that the EIT system can effectively simulate and detect tissue impedance variations, making it a promising tool for medical diagnostics. Future research should focus on integrating machine learning algorithms to further improve image reconstruction accuracy in EIT. In addition, the development of real-time processing systems is essential for clinical applications, ensuring faster and more efficient thoracic conductivity imaging. Expanding the dataset to include different types of tissue phantoms and testing under diverse environmental conditions will improve the durability and generalizability of the system. Advancing these aspects will contribute to a more reliable and clinically viable EIT imaging system, ultimately improving diagnostic capabilities and medical decision-making in thoracic health.

Corresponding author: Khusnul Ain, k_ain@fst.unair.ac.id, Department of Biomedical Engineering, Universitas Airlangga, Surabaya, Indonesia
DOI: https://doi.org/10.35882/ijeeemi.v7i2.54

REFERENCES

[1] A. Pulumati, A. Pulumati, B. S. Dwarakanath, A. Verma, and R. V. L. Papineni, "Technological advancements in cancer diagnostics: Improvements and limitations," *Cancer Rep.*, vol. 6, no. 2, pp. 1–17, 2023, doi: 10.1002/cnr2.1764.

[2] C. Dimas, V. Alimisis, N. Uzunoglu, and P. P. Sotiriadis, "Advances in Electrical Impedance Tomography Inverse Problem Solution Methods: From Traditional Regularization to Deep Learning," *IEEE Access*, vol. 12, no. March, pp. 47797–47829, 2024, doi: 10.1109/ACCESS.2024.3382939.

[3] K. Ain, O. N. Rahma, A. P. Putra, N. Syavinas, D. Darmawan, and H. Sohal, "Bone fracture detection using electrical impedance tomography based on STEMlab Red Pitaya," *Indones. J. Electr. Eng. Comput. Sci.*, vol. 32, no. 1, pp. 150–159, 2023, doi: 10.11591/ijeecs.v32.i1.pp150-159.

[4] T. K. Bera, J. Nagaraju, and G. Lubineau, "Electrical impedance spectroscopy (EIS)-based evaluation of biological tissue phantoms to study multifrequency electrical impedance tomography (Mf-EIT) systems," *J. Vis.*, vol. 19, no. 4, pp. 691–713, 2016, doi: 10.1007/s12650-016-0351-0.

[5] S. Mansouri, Y. Alharbi, F. Haddad, S. Chabcoub, A. Alshrouf, and A. A. Abd-Elghany, "Electrical Impedance tomography – Recent applications and developments," *J. Electr. Bioimpedance*, vol. 12, no. 1, pp. 50–62, 2021, doi: 10.2478/joeb-2021-0007.

[6] A. Roshanpanah, M. Abbasi, H. Attar, A. Amer, M. R. Khosravi, and A. A. Solyman, "An Electrical Impedance Imaging System Towards Edge Intelligence for Non-Destructive Testing of Concrete," *Tsinghua Sci. Technol.*, vol. 29, no. 3, pp. 883–896, 2024, doi: 10.26599/TST.2023.9010047.

[7] F. Pennati *et al.*, "Electrical Impedance Tomography: From the Traditional Design to the Novel Frontier of Wearables," *Sensors*, vol. 23, no. 3, 2023, doi: 10.3390/s23031182.

[8] H. Gagnon, M. Cousineau, A. Adler, and A. E. Hartinger, "A resistive mesh phantom for assessing the performance of EIT systems," *IEEE Trans. Biomed. Eng.*, vol. 57, no. 9, pp. 2257–2266, 2010, doi: 10.1109/TBME.2010.2052618.

[9] X. Zheng and G. Kou, "Research on EIT Image Reconstruction Based on Improved GREIT Algorithm," *ICSIDP 2019 - IEEE Int. Conf. Signal, Inf. Data Process. 2019*, no. 5, 2019, doi: 10.1109/ICSIDP47821.2019.9173497.

[10] B. F. de Moura, M. F. Martins, F. H. S. Palma, W. B. da Silva, J. A. Cabello, and R. Ramos, "Nonstationary bubble shape determination in Electrical Impedance Tomography combining Gauss–Newton Optimization with particle filter," *Meas. J. Int. Meas. Confed.*, vol. 186, no. June, p. 110216, 2021, doi: 10.1016/j.measurement.2021.110216.

[11] T. A. Khan and S. H. Ling, "Review on electrical impedance tomography: Artificial intelligence methods and its applications," *Algorithms*, vol. 12, no. 5, 2019, doi: 10.3390/a12050088.

[12] M. G. Crabb, "Convergence study of 2D forward problem of electrical impedance tomography with high-order finite elements," *Inverse Probl. Sci. Eng.*, vol. 25, no. 10, pp. 1397–1422, 2017, doi: 10.1080/17415977.2016.1255739.

[13] S. Liu, J. Jia, Y. D. Zhang, and Y. Yang, "Image Reconstruction in Electrical Impedance Tomography Based on Structure-Aware Sparse Bayesian Learning," *IEEE Trans. Med. Imaging*, vol. 37, no. 9, pp. 2090–2102, 2018, doi: 10.1109/TMI.2018.2816739.

[14] T. Gerasimenko *et al.*, "Impedance Spectroscopy as a Tool for Monitoring Performance in 3D Models of Epithelial Tissues," *Front. Bioeng. Biotechnol.*, vol. 7, no. January, 2020, doi: 10.3389/fbioe.2019.00474.

[15] C. G. Malmberg, "Electrical Conductivity of Dilute Solutions of "Sea Water" From 5 to 120 °C," *Phys. Chem.*, vol. 69, no. 1, 1965, [Online]. Available: http://nvlpubs.nist.gov/nistpubs/jres/69A/jresv69An1p39_A1b.pdf

[16] G. Rao, M. A. Sattar, R. Wajman, and L. Jackowska-Strumiłło, "Quantitative evaluations with 2d electrical resistance tomography in the low-conductivity solutions using 3d-printed phantoms and sucrose crystal agglomerate assessments," *Sensors (Switzerland)*, vol. 21, no. 2, pp. 1–31, 2021, doi: 10.3390/s21020564.

[17] M. Hayashi, "Temperature-electrical conductivity relation of water for environmental monitoring and geophysical data inversion," *Environ. Monit. Assess.*, vol. 96, no. 1–3, pp. 119–128, 2004, doi: 10.1023/B:EMAS.0000031719.83065.68.

[18] M. Pasha, S. Kupis, S. Ahmad, and T. Khan, "A Krylov subspace type method for Electrical Impedance Tomography," *ESAIM Math. Model. Numer. Anal.*, vol. 55, no. 6, pp. 2827–2847, 2021, doi: 10.1051/m2an/2021057.

[19] C. Dimas, N. Uzunoglu, and P. P. Sotiriadis, "A Parametric EIT System Spice Simulation with Phantom Equivalent Circuits," *Technologies*, vol. 8, no. 1, pp. 1–18, 2020, doi: 10.3390/technologies8010013.

[20] B. S. Lin, H. R. Yu, Y. T. Kuo, Y. W. Liu, H. Y. Chen, and B. S. Lin, "Wearable Electrical Impedance Tomography Belt With Dry Electrodes," *IEEE Trans. Biomed. Eng.*, vol. 69, no. 2, pp. 955–962, 2022, doi: 10.1109/TBME.2021.3110527.

[21] J. P. Agnelli, V. Kolehmainen, M. J. Lassas, P. Ola, and S. Siltanen, "Simultaneous Reconstruction of Conductivity, Boundary Shape, and Contact Impedances in Electrical Impedance Tomography," *SIAM J. Imaging Sci.*, vol. 14, no. 4, pp. 1407–1438, 2021, doi: 10.1137/21M1407975.

[22] Fei Yang and Jie Zhang and Patterson Robert,

Corresponding author: Khusnul Ain, k_ain@fst.unair.ac.id, Department of Biomedical Engineering, Universitas Airlangga, Surabaya, Indonesia
DOI: https://doi.org/10.35882/ijeeemi.v7i2.54

"MEFS - MIND electrical impedance tomography forward solver," *2010 Annu. Int. Conf. IEEE Eng. Med. Biol.*, pp. 1–23, 2010, doi: 10.1109/IEMBS.2010.5627164.

[23] D. Hu, K. Lu, and Y. Yang, "Image reconstruction for electrical impedance tomography based on spatial invariant feature maps and convolutional neural network," *IST 2019 - IEEE Int. Conf. Imaging Syst. Tech. Proc.*, pp. 1–6, 2019, doi: 10.1109/IST48021.2019.9010151.

[24] S. J. Hamilton, A. Hänninen, A. Hauptmann, and V. Kolehmainen, "Beltrami-net: Domain-independent deep D-bar learning for absolute imaging with electrical impedance tomography (a-EIT)," *Physiol. Meas.*, vol. 40, no. 7, 2019, doi: 10.1088/1361-6579/ab21b2.

[25] A. Denker *et al.*, "Data-driven approaches for electrical impedance tomography image segmentation from partial boundary data," *Appl. Math. Mod. Challenges*, vol. 2, no. 2, pp. 119–139, 2024, doi: 10.3934/ammc.2024005.

[26] I. Hikmah, A. Rubiyanto, and Endarko, "Two-dimensional electrical impedance tomography (EIT) for characterization of body tissue using a gauss-newton algorithm," *J. Phys. Conf. Ser.*, vol. 1248, no. 1, 2019, doi: 10.1088/1742-6596/1248/1/012008.

[27] A. Adler *et al.*, "GREIT: A unified approach to 2D linear EIT reconstruction of lung images," *Physiol. Meas.*, vol. 30, no. 6, 2009, doi: 10.1088/0967-3334/30/6/S03.

[28] Z. Liu and Y. Yang, "Multimodal Image Reconstruction of Electrical Impedance Tomography Using Kernel Method," *IEEE Trans. Instrum. Meas.*, vol. 71, 2022, doi: 10.1109/TIM.2021.3132830.

[29] X. Chen *et al.*, "Deep Autoencoder Imaging Method for Electrical Impedance Tomography," *IEEE Trans. Instrum. Meas.*, vol. 70, no. July 2021, 2021, doi: 10.1109/TIM.2021.3094834.

[30] M. G. Hanna *et al.*, "Future of Artificial Intelligence—Machine Learning Trends in Pathology and Medicine," *Mod. Pathol.*, vol. 38, no. 4, p. 100705, 2025, doi: 10.1016/j.modpat.2025.100705.

AUTHOR BIOGRAPHY

Rohadatul Aisya received a Bachelor's degree in Physics Education from Universitas Negeri Yogyakarta and is currently pursuing a Master's degree in Biomedical Engineering at Universitas Airlangga. She has a strong interest in medical instrumentation and research on diagnostic devices based on impedance spectroscopy, including Electrical Impedance Tomography (EIT) and Electrical Impedance Spectroscopy (EIS). Her research focuses on developing advanced methods to enhance medical imaging and diagnostic accuracy, particularly through computational techniques for image reconstruction. With an interdisciplinary approach, Aisya aims to contribute to the advancement of biomedical technology and digital health, improving healthcare accessibility and diagnostic precision in various medical applications.

Syifa Candiki Samatha received her Bachelor's degree in Biomedical Engineering from Airlangga University in 2024 and has been pursuing a fast-track Master's degree program since 2023, with an expected completion in 2025. Her thesis research focuses on biomechanical design and material simulation. She has a strong interest in the application of engineering and biomaterial in medicine and business, aiming to develop innovative solutions for improved patient care and medical outcomes while ensuring that these technologies reach those in need. With her dedication to interdisciplinary research, Candiki aspires to actively contribute to advancements in medical technology and support the development of the medical field through technology.

Khusnul Ain Prof. Dr. Khusnul Ain, S.T., M.Si. is a professor of biomedical engineering at Universitas Airlangga, specializing in Electrical Impedance Tomography (EIT) and Electrical Impedance Spectroscopy (EIS). He earned his Bachelor's and Master's degrees from Universitas Gadjah Mada and a Doctorate from Institut Teknologi Bandung. His research focuses on improving EIT image reconstruction with machine learning, biomedical signal processing, and IoT-based healthcare systems. Committed to advancing medical diagnostics, he integrates physics, computing, and engineering to develop non-invasive imaging technologies. Through interdisciplinary research, Prof. Khusnul Ain continues to enhance the accuracy and accessibility of biomedical engineering solutions for better healthcare outcomes.

Suryani Dyah Astuti Prof. Dr. Suryani Dyah Astuti, S.Si., M.Si., is the first professor in the field of biophysics at Airlangga University. She earned her Bachelor's degree from Gadjah Mada University, her Master's degree from the Bandung Institute of Technology, and her Doctorate from Airlangga University. Her research focuses on antimicrobial photodynamic therapy and the development of photonics-based medical instruments for therapy and

Corresponding author: Khusnul Ain, k_ain@fst.unair.ac.id, Department of Biomedical Engineering, Universitas Airlangga, Surabaya, Indonesia
DOI: https://doi.org/10.35882/ijeeemi.v7i2.54

biomodulation. Through these innovations, she contributes to the treatment of chronic diseases and biofilm infections. In recognition of her dedication, she has received various awards, including being named an inspirational figure in human rights and women's protection in the field of innovation.

Corresponding author: Khusnul Ain, k_ain@fst.unair.ac.id, Department of Biomedical Engineering, Universitas Airlangga, Surabaya, Indonesia
DOI: https://doi.org/10.35882/ijeeemi.v7i2.54